Crystal Structure and Electronic Characterization of *trans*- and *cis*-Perinone Pigments

Jin Mizuguchi

Department of Applied Physics, Graduate School of Engineering, Yokohama National University, 240-8501 Yokohama, Japan

Received: December 31, 2003

Perinones derivatives are industrially important pigments that exhibit shades in the solid state from red to bordeaux. Two representative derivatives are trans and cis isomers characterized by a clean reddish shade of orange (Pigment Orange 43) and bluish red (Pigment Red 194), respectively. The color generation mechanism has therefore been investigated in these compounds with special attention to the crystal structure and intermolecular interactions. The color in the solid state is determined by molecular absorption bands as well as additional bands at longer wavelengths due to excitonic interactions between transition dipoles. Especially, the molecule pairs along the stacking axis are found to play an important role in the determination of colors, giving rise to the clean orange of PO43 and bluish red of PR194.

1. Introduction

Perinone and perylene compounds are well-known industrially important pigments.[1] Both are chemically related. Perinone compounds are derived from naphthalene-1,4,5,8-tetracarboxylic acid, whereas perylenes are derivatives of perylene-3,4,9,10-tetracarboxylic acid. However, perinones have much less commercial impact as compared with perylenes, which offer a variety of commercial products from vivid red, via maroon to black. Only two perinone compounds have gained commercial importance: trans and cis isomers of the derivative (shown in Figure 1). The trans isomer (Pigment Orange 43 abbreviated to PO43) exhibits a clean reddish shade of orange, as shown in the diffuse reflectance spectrum (Figure 2) characterized by a steep absorption edge around 570 nm. On the other hand, the cis isomer (Pigment Red 194 abbreviated to PR194) affords a very dull, bluish red, as shown in Figure 2. Therefore, the former has much more commercial impact than the latter.

We have recently reported the crystal structure of PO43[2] and PR194.[3] PO43 is found to be isomorphous with PR194. The lattice parameters are quite similar except for angle β: 96.816(9)° in PO43 and 102.98(2)° in PR194. Nevertheless, the colors are distinctly different from each other. For this reason, we have attempted in the present investigation to elucidate the color generation mechanism of the trans and cis isomers from the standpoint of the crystal structure and intermolecular interactions.

2. Experimental Section

2.1. Materials. PO43 and PR194 were obtained from Clariant GmbH and purified by sublimation under argon at 675 K using a two-zone furnace.[4] Single crystals of PO43 were then grown from the vapor phase in a closed system at 693 K. After 36 h, a number of needle-shaped crystals were obtained. Similarly, single crystals of PR194 were also obtained in the form of needles. Both single crystals were used for structure analysis as well as for measurements of polarized reflection spectra.

Evaporated thin films of PO43 and PR194 were prepared on plain glass slides (film thickness: about 1000 Å) using conventional vacuum equipment (Tokyo Vacuum Co. Ltd.: model EG240). The evaporated films were exposed to the vapors of an organic solvent such as acetone to bring about spectral changes due to molecular rearrangement. Acetone vapor, for example, loosens the crystal lattice, thus allowing the molecules to slide and/or rotate to find energetically more stable sites.

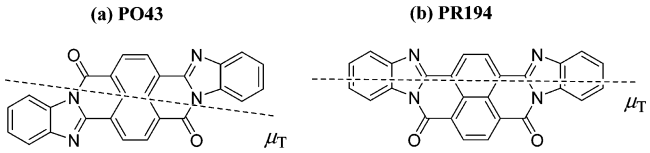

Figure 1. Molecular conformation: (a) PO43 (trans form) and (b) PR194 (cis form). The direction of the transition dipole (μ_T) is depicted in dashed lines.

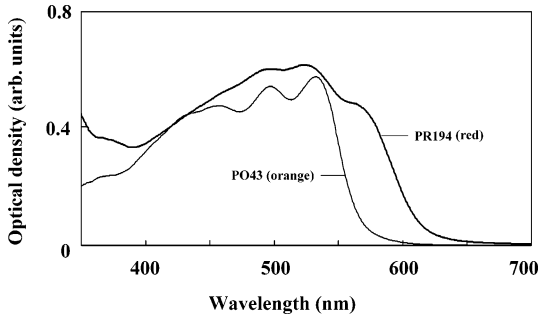

Figure 2. Diffuse reflectance spectra of PO43 and PR194 measured on powders.

2.2. Measurements. UV−vis spectra were recorded on a UV-2400PC spectrophotometer (Shimadzu). The temperature dependence of the absorption spectra in evaporated films was measured in the range between 20 and 300 K on a UV-2400PC spectrophotometer in combination with a cryostat from Iwatani Gas Co. Ltd. (model: CRT-105-OP). Diffuse reflectance spectra for powdered pigments were measured on a UV-2400PC spectrophotometer together with an integrating sphere attachment (ISR-240A from Shimadzu). Measurements for polarized reflection spectra were made on single crystals by means of a UMSP80 microscope-spectrophotometer (Carl Zeiss). An Epiplan Pol (×8) objective was used together with a Nicol-type polarizer. Reflectivities were corrected relative to the reflection standard of silicon carbide.

10.1021/jp031351d CCC: $27.50
Published on Web 05/27/2004

TABLE 1: Crystallographic Parameters for PO43 and PR194

	PO43	PR194
formula	$C_{26}H_{12}N_4O_2$	$C_{26}H_{12}N_4O_2$
crystal system	monoclinic	monoclinic
space group	$P2_1/c$	$P2_1/c$
molecular symmetry	C_i	C_{2v}
a (Å)	11.199(1)	12.423(3)
b (Å)	4.8120(6)	4.722(1)
c (Å)	16.091(2)	16.110(4)
β (deg)	96.816(9)	102.98(2)
V (Å^3)	861.0	920.9
Z	2	2
density (g/cm^3)	1.591	1.487

2.3. Molecular Orbital (MO) Calculation. The geometry of the molecules of PO43 and PR194 were optimized by means of AM1 Hamiltonian of MOPAC program package.[5] The INDO/S program used for spectroscopic calculations is part of the ZINDO program package.[6]

3. Results and Discussion

3.1. X-ray Structure Analysis. Table 1 details the crystallographic parameters for PO43[2] and PR194.[3] In both structures, the crystal system and space group are monoclinic and $P2_1/c$, respectively. The molecular symmetry is C_i for PO43 and C_{2v} for PR194 because of the disordered structure at the corner of the molecules (see ref 3 for details). PO43 and PR194 are isomorphous with each other, although angle β is slightly different: 96.816(9)° in PO43 and 102.98(2)° in PR194. The molecular arrangement as well as the overlap of two molecules along the stacking axis are shown in Figures 3 and 4 for PO43 and PR194, respectively. In both compounds, the molecules are arranged in a "hunter's fence" fashion when viewed from the *a*-axis. That is, on the (*a*, *c*) plane of PO43, the molecules of the first and third columns along the *a*-axis are all translationally equivalent. However, these are translationally inequivalent to the molecules of the second column. The molecules are alternately arranged along the (*a*, *c*)-diagonal direction in a fashion "upward and downward". Likewise, on the (*a*, *c*) plane of PR194, the molecules of the first and third columns along the *a*-axis are translationally equivalent, but translationally inequivalent to those of the second column.

3.2. MO Calculations of the Absorption Bands. Geometry optimization of MO calculations gave a heat of formation of 144.8 and 145.1 kcal/mol for PO43 and PR194, respectively. Both forms are, more or less, equally stable. The trans form has no dipole moment because of the C_i symmetry, whereas a small dipole moment of 0.07 D appears in the cis form perpendicular to the 2-fold axis of the C_{2v} symmetry. The spectroscopic calculations gave an absorption band around 416.2 nm with an oscillator strength of 1.180 in PO43; whereas the corresponding values for PR194 are 441.5 nm and 0.894, respectively. The direction of the transition dipole (μ_T) is given in Figure 1 in dashed lines. In both compounds, there is only one type of electronic transition in the visible region which is assigned to the HOMO/LUMO $\pi-\pi^*$ transition. It is to be noted that the absorption maximum in PO43 occurs at slightly shorter wavelengths than in PR194. This accords with experiment as described below.

3.3. Solution Spectra and Solid-State Spectra in Evaporated Films. Figure 5a and Figure 6a show the solution spectra of PO43 and PR194, respectively, together with those of evaporated, vapor-treated films. Likewise, Figures 5b and 6b show the temperature dependence of the absorption spectra in corresponding evaporated films measured in the temperature-range between 20 and 300 K.

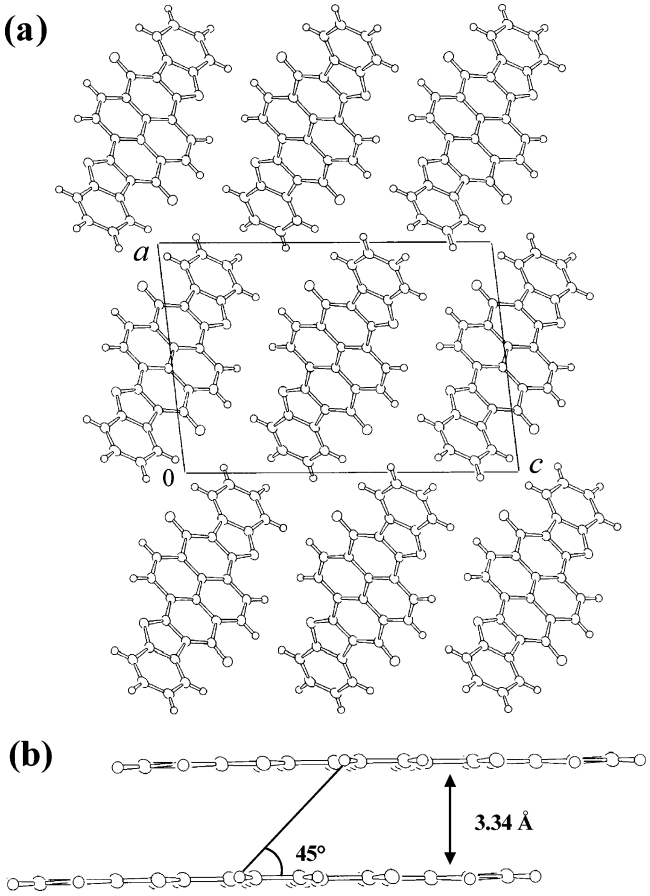

Figure 3. Molecular arrangement of PO43: (a) on the (*a*, *c*) plane and (b) along the stacking axis.

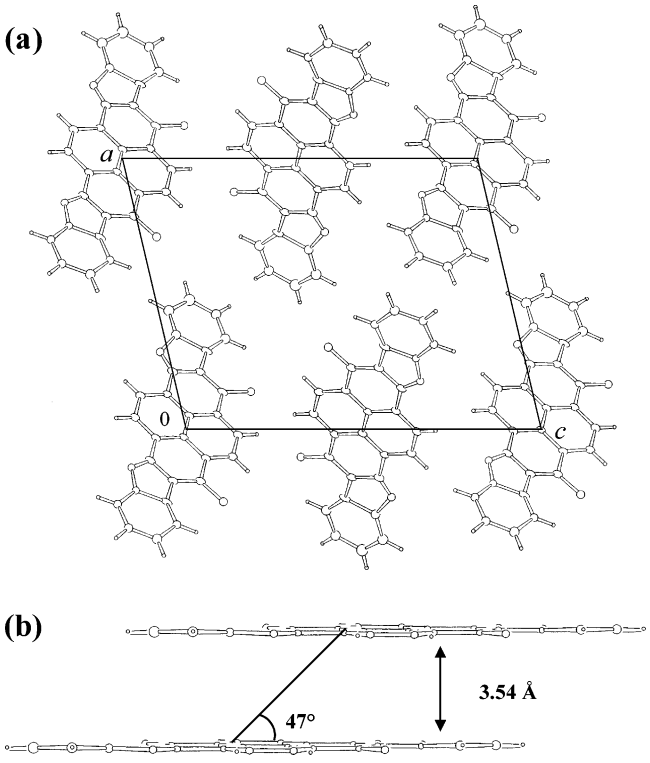

Figure 4. Molecular arrangement of PR194: (a) on the (*a*, *c*) plane and (b) along the stacking axis.

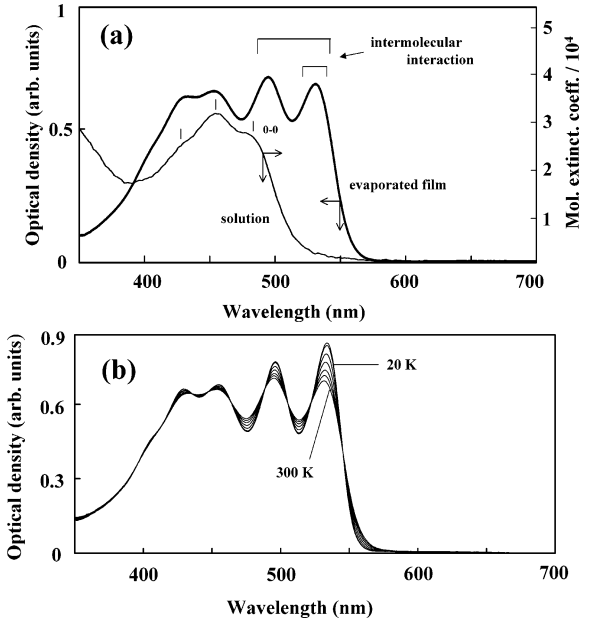

Figure 5. (a) Solution spectrum in dimethyl sulfoxide and solid-state spectrum in evaporated, vapor-treated films of PO43 and (b) temperature dependence of the absorption spectra in the range between 20 and 300 K.

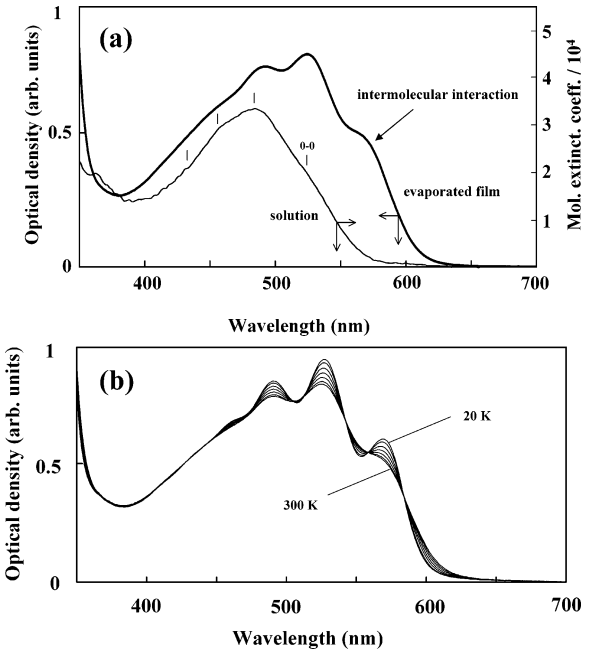

Figure 6. (a) Solution spectrum in dimethyl sulfoxide and solid-state spectrum in evaporated, vapor-treated films of PR194 and (b) temperature dependence of the absorption spectra in the range between 20 and 300 K.

First, we assign the molecular bands in solution. MO calculations revealed that, in both PO43 and PR194, there is only one sort of electronic absorption band in the visible region. This clearly indicates that the broad absorption bands in solution are attributed to vibronic bands (vibrational-electronic bands) arising from one electronic transition coupled with a series of vibrational transitions. Close examination of the spectrum for PO43 reveals that all absorption bands denoted by vertical, short lines are equally spaced (ca. 1200 cm^{-1}), indicating a progression of the absorption bands. The longest-wavelength band around 480 nm is then assigned to the pure electronic band and is designated by the 0−0 transition. The second longest wavelength band (around 455 nm) is attributed to the 0−1 transition in which the pure electronic transition is coupled with one vibrational transition of ca. 1200 cm^{-1}. Likewise, the incipient band round 430 nm is assigned to the 0−2 transition. Similarly, in PR194, the absorption shoulder (i.e., incipient band) around 535 nm is assigned to the 0−0 transition, followed by the 0−1, 0−2, and 0−3 transitions. The longest-wavelength band in PO43 (480 nm) appears at shorter wavelengths than that of PR194 (535 nm). This tendency agrees with the MO calculations.

Next, we look at the solid-state spectra in evaporated films and compare them with those of the solution spectra. It is important to note that the number of absorption bands is increased on going from solution to the solid state. We discuss first the absorption bands of PR194, because the assignment is straightforward. All absorption bands in solution are slightly displaced on going from the solution to the solid state. Nevertheless, one-to-one correspondence of the absorption bands between the solution and solid state is possible except for the longest wavelength shoulder (i.e., incipient band: 565 nm) in the solid state. Because this band cannot be assigned on the basis of the molecular bands in solution, it is obviously attributed to a band caused by intermolecular interactions upon crystallization. In addition, the present shoulder grows up to an absorption band at 20 K (Figure 6b), accompanied by several isosbestic points. The absorption spectrum at 20 K resembles the diffuse reflectance spectrum shown in Figure 2.

The assignment of the absorption bands in PO43 is more complicated. The absorption tail around 350 nm in solution cannot be observed in evaporated films (Figure 5a). If we assume it to be a hypsochromic shift upon crystallization, then the 0−0 band (480 nm) in solution corresponds to the band around 460 nm in evaporated films, accompanied by a progression of the equally spaced bands around 425 nm (0−1 transition) and 405 nm (0−2 transition). This means that two additional bands appear upon crystallization: 495 and 530 nm. Both bands exhibit significant temperature dependence at low temperatures, as presumably caused by enhanced intermolecular interactions due to lattice contraction at low temperatures. Here again, the absorption spectrum at 20 K is quite similar in shape to the diffuse reflectance spectrum shown in Figure 2.

Apart from the above assignment, it is also likely that only the longest-wavelength band around 530 nm is attributed to a band due to intermolecular interactions, just as in PR194. In this case, the spacing between vibronic bands is not equal, making the assignment difficult. It follows that no clear-cut explanation is available on the basis of the present experimental results. Nevertheless, it is safe to say that, at least, one additional band appears as a result of intermolecular interactions on going from the solution to the solid state.

3.4. Polarized Reflection Spectra Measured on Single Crystals and Resonance Interactions between Transition Dipoles. Figures 7 and 8 show the polarized reflection spectra measured on the (*b*, *c*) plane of single crystals of PO43 and PR194 together with their corresponding projections, respectively. The direction of the transition dipole of the molecules for PO43 and PR194 is shown in Figure 1 and is along the long-molecular axis. On the (*b*, *c*) plane of PO43, there are two types of molecular orientations: translationally equivalent and translationally inequivalent molecules. The projection of the corresponding transition dipoles is larger onto the *b*-axis than onto the axis perpendicular to it (i.e., *c*-axis). This indicates that the molecules are more favorably excited for polarization parallel to the *b*-axis than perpendicular to it. This is well reflected in the polarized reflection spectra, showing higher

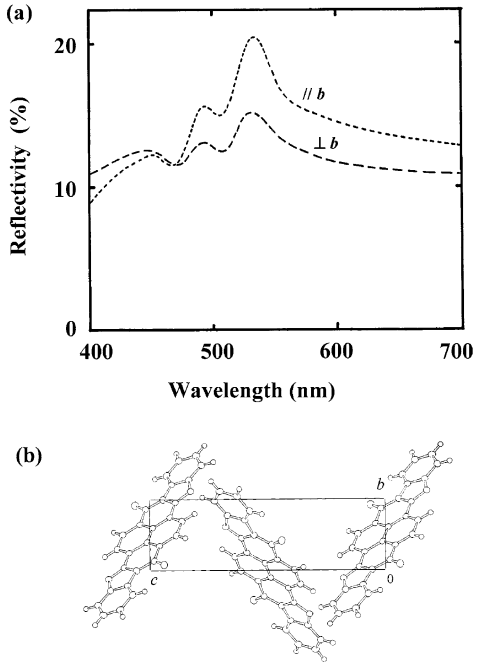

Figure 7. (a) Polarized reflection spectra measured on the (*b*, *c*) plane of single crystals of PO43 and (b) the projection of the crystal structure onto the (*b*, *c*) plane.

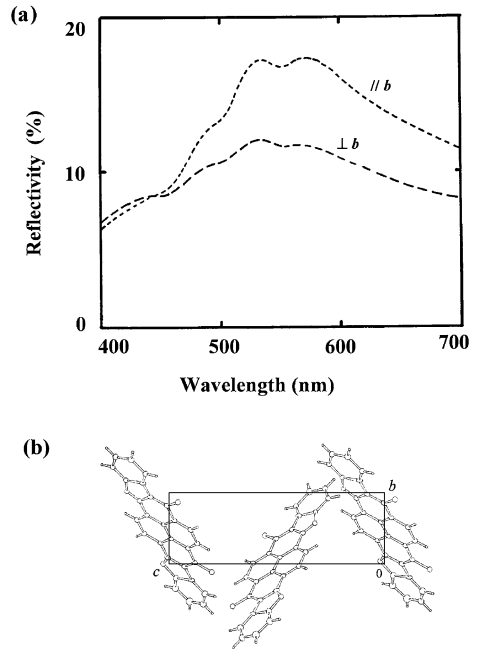

Figure 8. (a) Polarized reflection spectra measured on the (*b*, *c*) plane of single crystals of PR194 and (b) the projection of the crystal structure onto the (*b*, *c*) plane.

reflectivity with parallel polarization than with perpendicular polarization. The present reflection spectra are basically in good accord with the diffuse reflection spectrum (Figure 2) and the absorption spectrum of evaporated films (Figure 5).

It is also important to note that the three reflection bands in the visible region (Figure 7a) are equally intensified, or less intensified for different polarizations. This indicates that all reflection bands are attributed to one single electronic transition, as also supported by MO calculations. In addition, the position of the reflection maximum at the longest-wavelength is slightly different for different polarizations. This is due to the Davydov splitting[7,8] caused by excitonic interactions between translationally inequivalent transition dipoles (Figure 7b). The presence of the Davydov splitting indicates that the excitonic interactions are also operative between translationally equivalent transition dipoles to displace the absorption bands toward longer or shorter wavelengths as discussed below.

A similar spectroscopic result is also obtained for PR194, as shown in Figure 8. Polarization parallel to the *b*-axis is more favored (i.e., higher reflection) for excitation of the molecules than perpendicular to the *b*-axis. In addition, the Davydov splitting is also observed due to translationally inequivalent transition dipoles (Figure 8b). The reflection spectra are in good agreement with the diffuse reflectance spectrum (Figure 2) and the absorption spectrum of evaporated films (Figure 6).

3.5. Assignment of the Long-Wavelength Band in PO43 and PR194. When an excitation induces a transition dipole in the molecule, the excited state in crystals involves wave functions with significant probabilities on nearest neighbors. Therefore, the exciton coupling may well involve energy contributions from interactions with all of these nearest neighbor molecules acting in concert in the lattice. This may lead to the band splitting (Davydov splitting) of the excited state or spectral displacement toward longer or shorter wavelengths. The interaction energy ($\Delta E_{\text{exciton}}$) is given by the dipole−dipole equation:[7,8] $\Delta E_{\text{exciton}} = |\mu_T|^2(1 - 3\cos^2\theta)/r^3$, where the transition dipole is denoted by μ_T and the distance and angle between two transition dipoles are denoted by r and θ, respectively. As evident from the present equation, the overall spread or shift energy is determined by the strength of the interneighbor coupling ($|\mu_T|^2$), which directly depends on the absorption coefficient of the molecule as well as on the mutual relative orientation of the transition dipoles in molecular assemblies. That is, the term $(1 - 3\cos^2\theta)/r^3$ determines the geometrical relationship of transition dipoles correlated with the crystal structure. Because this term falls off as the inverse cube of distance, most of the interaction would come from the nearest neighbors. The bathochromic or hypsochromic shift depends on the critical angle of $\theta = 54.7°$, below which the former will result and above which the latter will be the case. The present excitonic interaction is especially significant in dyestuff or pigment systems[9−11] because their absorption coefficients are quite large.

On the basis of the above exciton theory, we interpret the longest-wavelength band in PO43 and PR194 as arising from excitonic interactions in consideration of the direction of the transition dipole (Figure 1) and the molecular arrangement (Figures 3 and 4). This is a crude estimate, but it is of great help for developing an understanding of the electronic structure. The molecule pairs on the molecular plane as well as along the stacking axis are involved in spectral shifts. For example, on the (*a*, *c*) plane of PO43 (Figure 3a), the angle and distance of horizontally arranged (translationally equivalent) molecule pairs as well as those of vertically arranged ones are about 82° and 16.1 Å and 17° and 11.2 Å, respectively. The diagonal molecule-pairs are translationally inequivalent. On the other hand, the stack pair (Figure 3b) is arranged with an angle of 45° and with an interplanar distance of about 3.34 Å. Simple calculation of the geometrical term $(1 - 3\cos^2\theta)/r^3$ reveals that the bathochromic contribution of the stack pair is about 1 order of magnitude larger than that on the molecular plane. Therefore, the bathochromic displacement is mainly caused by the stack pair in PO43. Similarly, on the (*a*, *c*) plane of PR 194 (Figure 4a), the angle and distance between transition dipoles of the horizontally arranged (translationally equivalent) pairs are 82° and 16.1 Å, respectively, whereas those of vertical pairs are

28° and 12.4 Å. The diagonal pairs are translationally inequivalent. On the other hand, in the stack pair (Figure 4b), the angle and interplanar distance are about 47° and 3.45 Å, respectively. Here again, the stack pair contributes more significantly to the bathochromic shift by 1 order of magnitude than those on the molecular plane.

In summary, an additional band (or bands) appears in PO43 and PR194 upon crystallization because of excitonic interactions between transition dipoles in stack pairs. This plays an important role in the determination of the color in the solid state together with individual molecular absorption bands.

4. Conclusions

The color generation mechanism of PO43 and PR194 has been investigated with major focus on the crystal structure and intermolecular interactions. PO43 and PR194 are isomorphous to each other, but the molecular arrangement and the direction of the transition dipoles are slightly different. In both compounds, an additional absorption band (or bands) appears at longer wavelengths upon crystallization due to excitonic interactions between transition dipoles. These bands play an important role in the determination of the shade of PO43 and PR194 in the solid state.

Acknowledgment. I express my sincere thanks to Mr. H. Shikamori for experimental assistance.

References and Notes

(1) Herbst, M.; Hunger, K. *Industrial Organic Pigments*; VCH: New York, 1993.
(2) Mizuguchi, J. *Z. Kristallogr. NCS* **2003**, *218*, 137.
(3) Mizuguchi, J. *Z. Kristallogr. NCS* **2003**, *218*, 139.
(4) Mizuguchi, J. *Krist. Technol.* **1981**, *16*, 695.
(5) WinMOPAC Ver.3, Fujitsu.
(6) Zerner, M. C. ZINDO, A General Semiempirical Program Package. Department of Chemistry, University of Florida, Gainesville, FL.
(7) Kasha, M. *Spectroscopy of the Excited State*; Plenum Press: New York, 1976; p 337.
(8) Craig, D. P.; Walmsley, S. H. *Excitons in Molecular Crystals*; W. A. Benjamin, Inc.: Reading, MA, 1968.
(9) Endo, A.; Matsumoto, S.; Mizuguchi, J. *J. Phys. Chem. A* **1999**, *103*, 8193.
(10) Mizuguchi, J. *J. Phys. Chem. A* **2000**, *104*, 1817.
(11) Mizuguchi, J.; Tojo, K. *J. Phys. Chem. B* **2002**, *106*, 767.